Geofísica Internacional 47 (3), 301-310 (2008)

Transport in the interplanetary medium of coronal mass ejections

A. Borgazzi[1*], A. Lara[2], L. Romero-Salazar[3] and A. Ventura[2,3]
[1]*Divisão de Geofísica Espacial, Instituto Nacional de Pesquisas Espaciais, São Jose dos Campos, São Paulo, Brazil.*
[2]*Instituto de Geofísica, Universidad Nacional Autónoma de México, Mexico City, Mexico*
[3]*Facultad de Ciencias, Universidad Autónoma del Estado de México, Mexico*

Received: November 3, 2007; accepted: May 23, 2008

Resumen

Las eyecciones de masa coronal (EMCs) son estructuras de plasma y campo magnético expulsadas desde el Sol hacia el medio interplanetario y generalmente observadas coronógrafos de luz blanca. Durante su viaje, estas estructuras, ahora llamadas eyecciones de masa coronales interplanetarias (EMCIs) sufren aceleración o desaceleración debido a la interacción con el viento solar circundante. Este proceso puede ser entendido como una transferencia de momento entre la EMCI y el viento solar siendo esta transferencia diferente en el caso de las EMCIs 'rápidas' y las EMCIs 'lentas' (comparando su velocidad con la del viento solar).

Desde el punto de vista de la dinámica de fluidos, estamos interesados en estudiar el comportamiento de esta transferencia de momento considerando a la EMCI y el viento solar como la interacción de dos fluidos, aplicando la idea de esfuerzo viscoso, tomado en cuenta que, en este caso especial estamos tratando con interacción viscosa entre plasmas de baja densidad. Hemos resuelto para las EMCIs 'rapidas', la Segunda Ley de Newton considerando fuerzas viscosas, obteniendo una solución exacta para la velocidad de las EMCIs en función del tiempo. Se comparan los resultados analíticos con algunos modelos empíricos presentes en la literatura, y se sugieren valores para el coeficiente de viscosidad y arrastre en este sistema. Es importante mencionar que los resultados presentados, en esta primera aproximación, han sido obtenidos sin la presencia de un término que considere el campo magnético.

Palabras clave: Eyecciones de masa coronal, clima espacial

Abstract

Coronal mass ejections (CMEs) are large scale structures of plasma and magnetic field expelled from the Sun to the interplanetary medium and generally observed in white light coronagraphs. During their travel, in the interplanetary medium these structures named interplanetary coronal mass ejections (ICMEs), suffer acceleration or deceleration due to the interaction with the ambient solar wind. This process can be understood as a transference of momentum between the interplanetary CME (ICME) and the solar wind. This process seems to be fundamentally different for 'slow' and 'fast' ICMEs (compared with the ambient solar wind velocity).

In this work, we approach the problem from the fluid dynamics point of view and consider the ICMEs - solar wind system as two interacting fluids under the action of viscous forces. We note that this interaction is a special case of interaction between low density plasmas. Using these viscous forces in the Newtons Second Law, we obtained an analytical solution for the ICME velocity as a function of time. By comparing our analytic results with empirical models found in recent literature, we suggested values for the viscosity and drag parameters in this system. In this first approximation we have neglected the magnetic field.

Key words: Coronal mass ejections, space weather, ICME travel time.

Introduction

Coronal mass ejections (CMEs) are one of the major forms of solar activity that inject mass and energy into the interplanetary space. In average CMEs have a mass of 10^{16} g and cover a wide range of speeds, from ~100 km/s to ~ 3000 km/s (Gosling *et al.*,1991; St. Cyr *et al.*,1999).

Depending on their direction of propagation, some of these interplanetary CMEs (ICMEs) impact the Earth's magnetosphere. The disturbance caused in the Earth's environment depends on the ICME structure: as the exerted by the ICME on the magnetosphere strength and direction of the magnetic field, as well as the dynamical pressure (Gonzalez *et al.*,1999). Therefore, these parameters are

important for the space weather and magnetospheric physics. In terms of space weather prediction, a very important parameter is the ICME arrival time, or in other words, the Sun-Earth ICME travel time. This travel time depends on the CME initial velocity and the ICME - solar wind (SW) interaction, (see Cargill, 2004 and references therein).

Fast ICMEs (V_{cme} > 400 km/s) undergo a deceleration because of thin interaction with the solar wind, with the corresponding diminishing of its velocity down to the solar wind velocity. On the other hand, slow ICMEs (V_{cme}< 400 km/s) are accelerated, increasing their velocity from its initial value up to the ambient SW velocity ~ 400 km/s (Gopalswamy *et al*., 2000; Gopalswamy *et al*., 2001). Many attempts have been done to quantify this interaction: using theoretical models, for example the work of Canto *et al*. (2005) describes the dynamics of a 'working surface' created by temperature, density and velocity fluctuations in the solar wind; empirical models as the series of works of Gopalswamy *et al*. (2000, 2001, 2005) which we use here to compare our model. Similar models were developed by Vršnak (2001, 2002, 2004, 2007) and Dal Lago *et al*. (2004); Howard *et al*. (2007); Lindsay *et al*. (1999); Schwenn *et al*. (2005); Webb *et al*. (2000, 2000a) Also simulations studies have been carried out (Cargill *et al*., 1996; Cargill, 2004; Vandas *et al*., 1995; Odstrčil *et al*., 1999; Odstrčil *et al*., 1999a; Odstrčil *et al*., 1999b).

In particular, Cargill, (2004) uses a similar approach than ours to the ICME dynamics, although, he use simulations to solve the magnetohydrodynamic equations. In a comparable study, but using 1D hydrodinamic simulations of a single fluid, González-Esparza *et al*. (2003) were capable of reproduce the ICME propagation by varing the initial CME and SW parameters.

In this work we use fluid dynamics theory to reproduce the ICME transport in the interplanetary medium. In particular we study the deceleration as a function of two viscous forces: 'laminar' and 'turbulent' viscous interactions.

The drag force

The force acting in a system of two immiscible liquids, like a drop of oil immersed in water, is due to the viscosity and is known as drag force. In fluid dynamics, the viscosity is a measure of the resistance to shear or angular deformation, and is due to the momentum interchange between the components of the fluids (Batchelor, 2000). In this example, the drop has a representative linear dimension 'd' (diameter) and is in steady translational motion with velocity 'U' in the medium. In this case, viscous forces are of the order of $\eta U/d^2$, where η is the viscosity of the medium. On the other hand, inertial forces are of the order of $\rho U^2/d$, where ρ is the density of the medium. The ratio of these forces ($\rho dU/\eta$=Re) is the Reynolds number (Re). For a small Reynolds number (Re << 1) the inertia forces may be negligible. We can consider this, as the 'laminar' case and the drag force is, (in the special case of a spherical body):

$$F_L = 6\pi R\eta U \tag{1}$$

In the case of high Reynolds number Re >>1 the viscous forces in the fluid may be negligible and the 'turbulent' drag forces take the form of:

$$F_T = \frac{C_d A\rho U^2}{2} \tag{2}$$

A and R are the area and radius of the (spherical) drop. C_d is another common feature that appears when describing the friction exerted over a moving body immersed in a fluid, is a dimensionless coefficient which represents the drag and basically depends on the shape of the immersed object. In this study, both 'laminar' and 'turbulent' forces are used in similar way as in the hydrodynamics theory. Whe note that in the case of collision-less fluids, the interchange of momentum may be due by means of waves or other collective microscopic plasma processes.

ICME SW interaction

In this approximation, we consider the ICME as a fluid moving inside another fluid (the SW) and affected by two viscous forces, 'laminar' (Equation 1) and 'turbulent' (Equation 2). The laminar or turbulent regime may apply depending on the difference of velocities; and/or the global ICME structure; and/or magnetic field configuration. As instance, the laminar case may apply when an ICME smoothly opens the current sheet and travels inside it; or in the case of a quasi-parallel shock (with respect to the ambient SW magnetic field). Whereas the turbulent case may apply to a quasi-perpendicular shock. The details of these interactions are out of the scope of this paper, therefore, in this approximation we assume these (magnetic) effects as enclosed in any of the two macroscopic regimes.

In this case, R is the ICME radius (assuming a spherical shape), which changes as a function of the traveled distance ($R = x^{0.78}$), η the SW 'viscosity' and U the ICME velocity, C_d is the drag coefficient, $A=\pi R^2$ is the ICME effective section and ρ_{sw} is the SW density. In a reference system where the 'fluid' (the ambient SW) is at rest, the ICME velocity is $U = U_{ICME} - U_{SW}$, here U_{SW} represents the solar wind velocity.

We model the friction or drag force under which the ICME is affected by means of Newton's Second Law (see Fig. 1) and considering the separate effects of both 'laminar' and 'turbulent' viscous forces, this leads us to the following differential equations:

$$-L_1 (U - U_{sw}) = m_{cme} \frac{d(U - U_{sw})}{dt} \quad (3)$$

where L1 = $6\pi R\eta$

$$-\frac{T_1(U - U_{SW})^2}{2} = m_{cme} \frac{d(U - U_{sw})}{dt} \quad (4)$$

where $T_1 = C_d A \rho_{sw}$

As we do not have an actual value of the Reynolds number in the interplanetary space we can explore the dynamics of the ICME through a total force constructed as the superposition of both laminar and turbulent effects. In other words we define the total drag force as Taylor's expansion up to the first two terms:

$$-L_1 (U - U_{sw}) - \frac{T_1(U - U_{SW})^2}{2} = m_{cme} \frac{d(U - U_{sw})}{dt} \quad (5)$$

The time solution of these equations are:

$$U = U_{sw} + (U^0_{CME} - U_{SW})\, e^{-\frac{L_1 t}{m_{cme}}} \quad (6)$$

$$U = U_{sw} + \frac{2m_{cme}(U^0_{CME} - U_{SW})}{T_1(U^0_{CME} - U_{SW})t + 2m_{cme}} \quad (7)$$

$$U = U_{sw} + \frac{2L_1(U^0_{CME} - U_{SW})}{[T_1(U^0_{CME} - U_{SW}) + 2L_1]e^{\frac{L_1 t}{m_{cme}}} - T_1(U^0_{CME} - U_{SW})} \quad (8)$$

Results

Upon inspection of the solutions given by equations 6 and 7 and comparing with experimental observations of the phenomena (Gopalswamy *et al*., 2000) we have identified extreme values for the viscosity and drag coefficient, η and C_d respectively. Such comparison was meant to recover the fast CMEs velocities near the proximity of the Sun (around 400 to almost 3000 km/s. Whereas near the Earth (i.e. at a distance of 1AU), the ICMEs velocities diminishes down to a range of 400 to 1000 km/s). The corresponding values for the viscosity and drag coefficient where $\eta_1 = 0.002$ *kg/ms* and $C_{d1} = 200$ for the minimum case; and $\eta_2 = 0.02$ *kg/ms* and $C_{d2} = 2000$ for the maximum drag effect. To analyze the motion described by our solutions (equation 6 and equation 7) we have plotted the resulting velocity versus time, for the two extreme cases mencioned abobe. Our results are plotted in Fig. 2 and Fig. 3, for 'laminar' and 'turbulent' ICME-SW interactions, respectively. Continuous lines in Fig. 2 represent the ICME dynamics in the 'laminar' regime using η_2 and dotted lines represent the same behavior but with η_1. At $t = 0$ the velocity is the initial CME velocity. The stars and triangles are the ICME arrival time at 1 AU, with η_2 and η_1 respectively. In Fig. 3 the continuous lines are the solutions of equation 7 under a drag coefficient of C_{d2} whereas the dotted lines are the solutions with C_{d1}.

In all cases we have used a mean SW density, $\rho_{sw} = 10$ *part/cm*^{3} a mean CME mass, $M_{cme} = 10^{16}$ *gr* and a mean

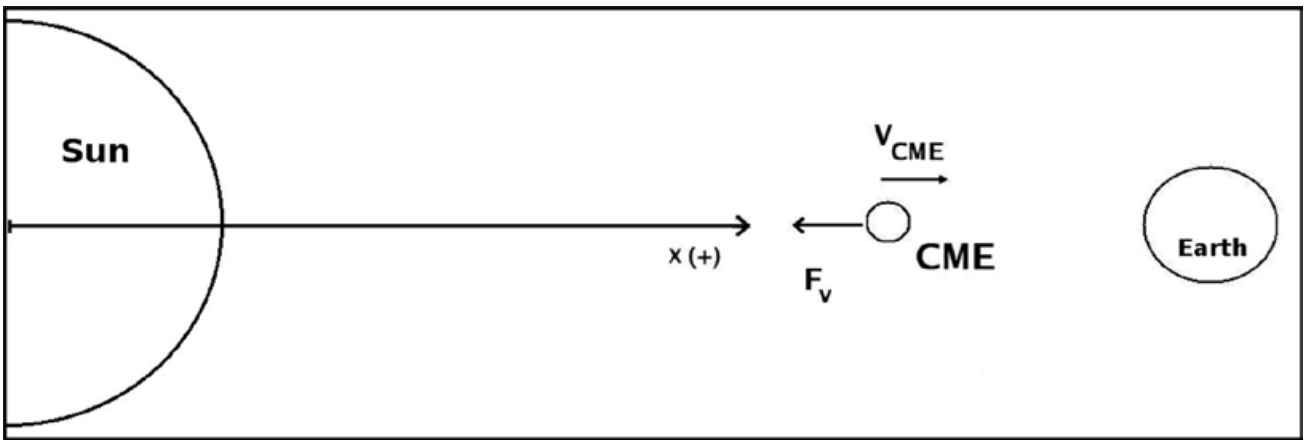

Fig. 1. Schematic representation of the total viscous force Fv which decelerates the ICME during the travel in the interplanetary space.

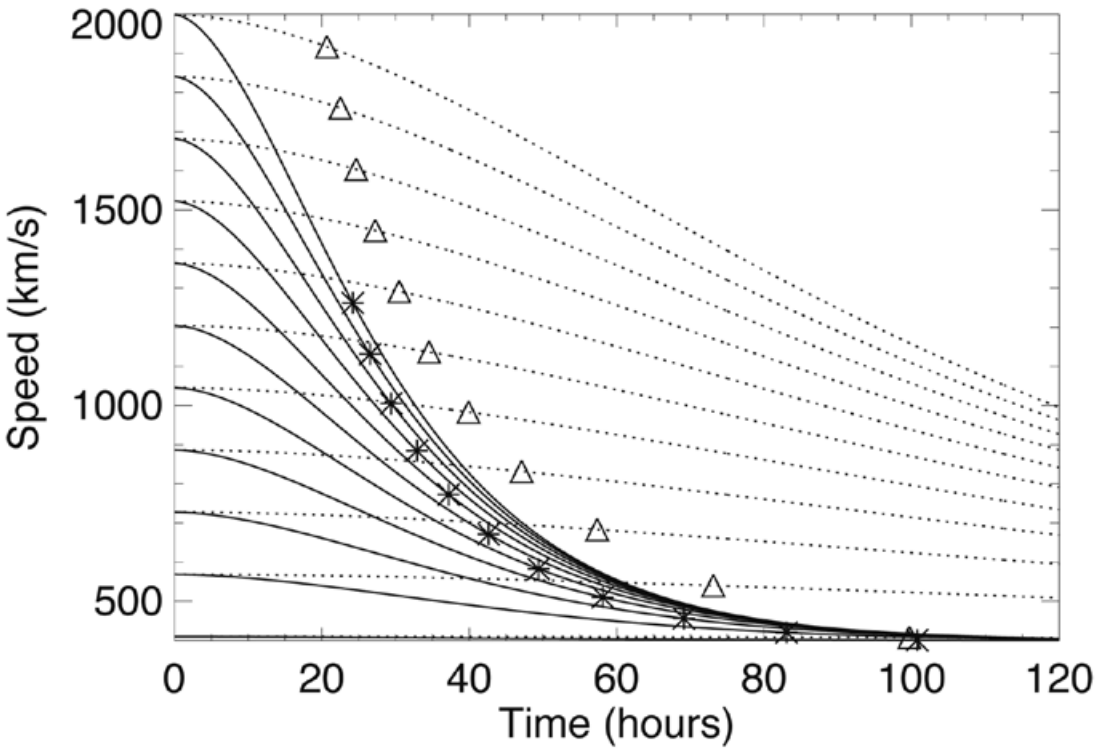

Fig. 2. Evolution of the ICMEs velocity in terms of the initial CME velocity under a ´laminar´ drag force. The dotted lines correspond to a viscous coefficient of 0.002 *kg*/*ms* and the continuous lines to 0.02*kg*/*ms*. The stars and triangles represent the travel time from the Sun to 1 AU.

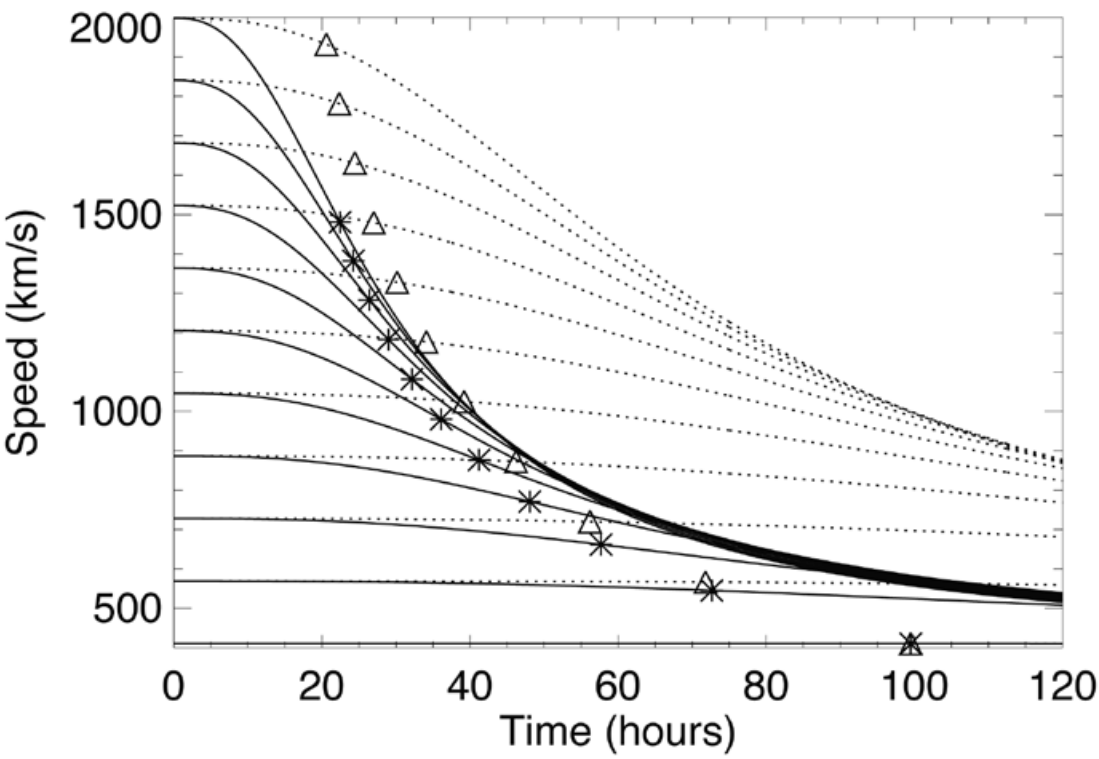

Fig. 3. Temporal behavior of the ICMEs velocity under a 'turbulent' drag force. The dotted lines correspond to a drag coefficient of 200 and the continuous lines correspond to a value of 2000.

SW velocity, V_{SW} = 400 *km/s*. Each line is the solution of the respective equation with different initial velocity (U_{CME}) ranging from 400 to 2000 *km/s*. Stars and triangles represents again the ICME arrival time at 1 AU.

In order to analyze the simultaneous effect of 'laminar' and 'turbulent' forces over the ICMEs velocity, we present in Fig. 4 a family of solutions of equation 8 for different initial velocity conditions. We note the emphasized damping effect occurring for the continuous line with respect to the dotted lines. We use the same convention of the stars and triangles as in previous plots.

Another interesting analysis of the CMEs speed behavior would be plotting this as a function of the traveled distance, in this way, we are able to compare our results with observations made at 1 AU. To compute the ICME velocity as a function of distance, we evaluate equations 6, 7 and 8 in 2400 time points from 0 to 431820 sec. (5 days), i. e., Δt = 180 sec. Then we compute the distance $\Delta x(\Delta t)$ assuming constant acceleration during each interval.

Figs. 5, 6 and 7 represent the behavior of the velocity as a function of distance for the ICMEs under the action of a 'laminar', 'turbulent' and coupled viscous forces, respectively. Here the difference between models and parameters are evident an ICME with an initial velocity of 2000 *km/s* will arrive at 1 AU with a velocity of 1900 *km/s* and 1250 *km/s* using η_1 and η_2, respectively. If the initial velocity is 900 *km/s* the velocities at 1 AU are 820 *km/s* and 510 *km/s*, respectively. For the turbulent case, the velocity at 1 AU is 1950 *km/s* using C_{d1} and 1500 *km/s* using C_{d2} for an initial velocity of 2000 *km/s*. If the initial velocity is 900 *km/s* the velocities at 1 AU are 880 *km/s* and 550 *km/s*, respectively.

In the coupled case, using η_1 and C_{d1}, the velocity at 1 AU is 1880 *km/s* if the initial velocity is 2000 *km/s* and 870 *km/s* if the initial velocity is 900 *km/s*. On the other hand, using η_2 and C_{d2}, the arrival velocity at 1 AU is 1000 *km/s* for an initial velocity of 2000 *km/s* and 550 *km/s* when the initial velocity is 900 *km/s*.

The minimum drag effect is reached when the force is laminar and $\eta = \eta_2$. An intermediate drag effect corresponds to the turbulent force and $C_d = C_{d2}$. The maximum drag effect is reached using the coupled force with $\eta = \eta_2$ and $C_d = C_{d2}$.

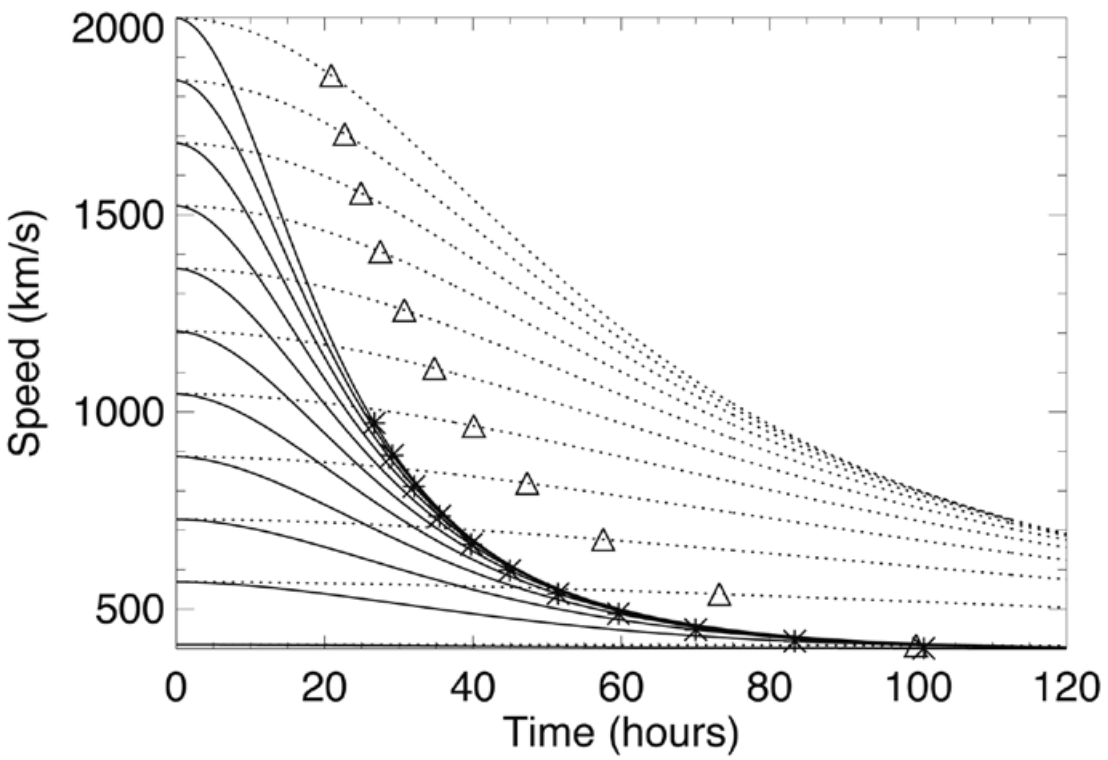

Fig. 4. ICMEs velocity in terms of time, for 'laminar' plus 'turbulent' forces. Dotted lines represent a drag and viscous coefficients of 200 and 0.002 *kg/ms* respectively, and continuous lines a drag coefficient of 2000 and a viscous coefficient of 0.02*kg/ms*.

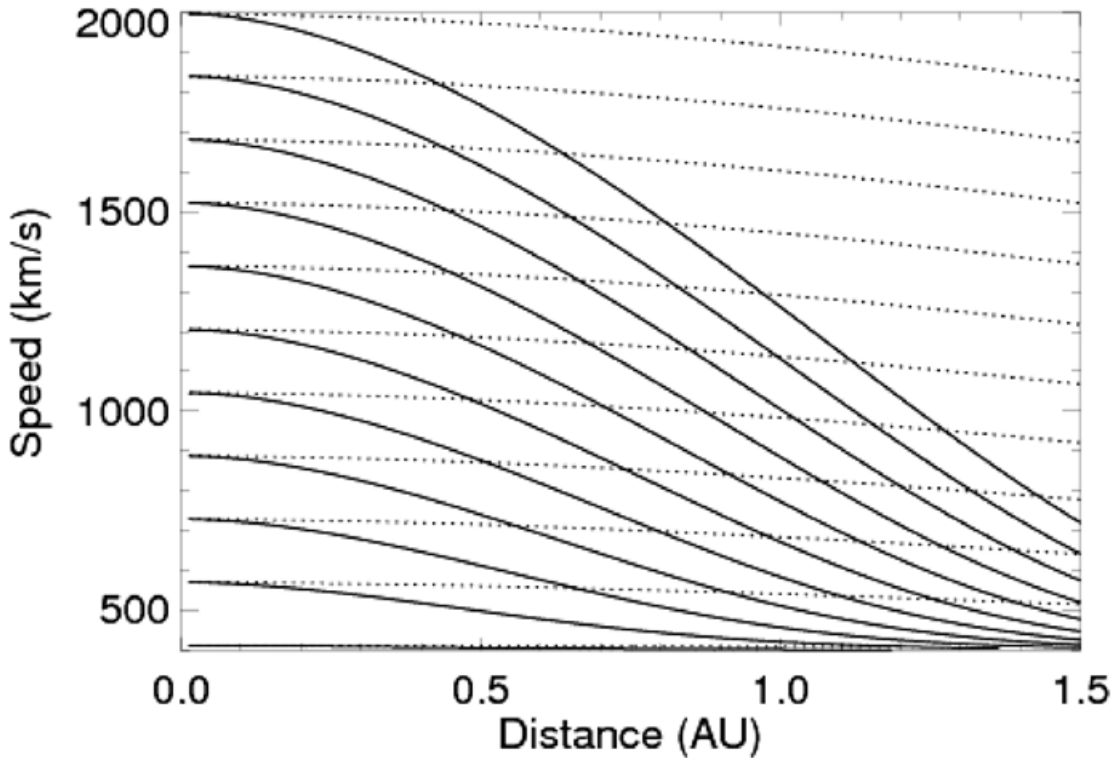

Fig. 5. ICME velocity in terms of the distance to the Sun for the 'laminar' interaction. Two cases are shown: the dotted lines represent the behavior using a viscous coefficient of 0.002 *kg/ms*, and the continuous lines with a coefficient of 0.02 *kg/ms*.

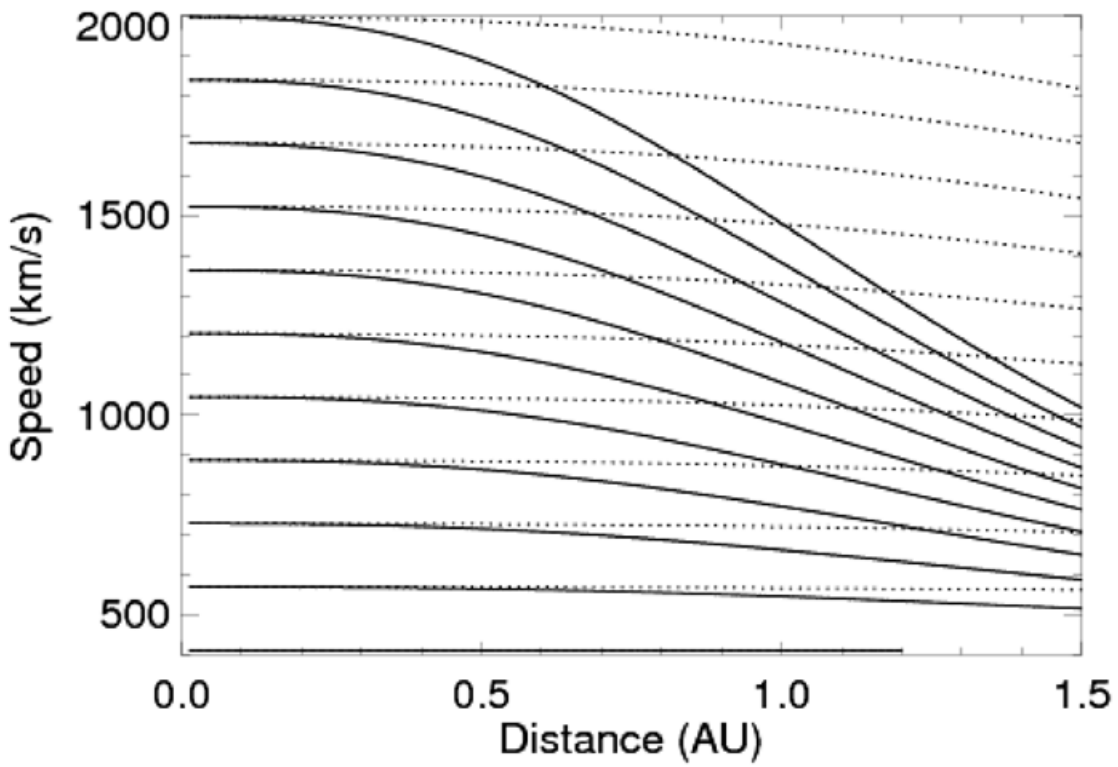

Fig. 6. Similar to Fig. 5 but for the 'turbulent' force. Dotted lines represent the behavior under a drag coefficient of 200, and the continuous lines with a coefficient of 2000.

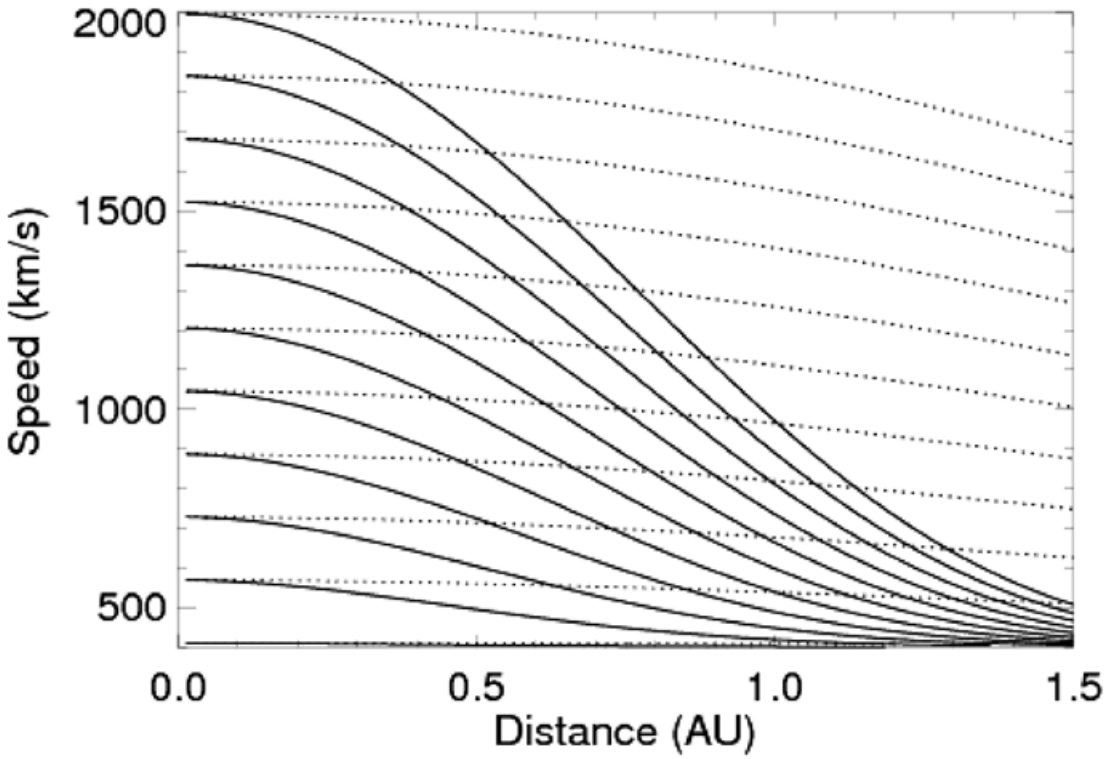

Fig. 7. Similar to Fig. 5 but for the 'laminar' plus 'turbulent' forces. Dotted lines represent the ICME behavior under a drag coefficient of 200 and a viscous coefficient of 0.002 *kg/ms*, and the continuous lines with a coefficient of 2000 and a viscous coefficient equal to 0.02 *kg/ms*.

ICME Travel time

The ICME travel time from the Sun to the Earth is an important parameter in terms of space weather prediction. Some empirical models have been proposed to predict the 1AU arrival time of coronal mass ejections. (Gopalswamy *et al*., 2000; Gopalswamy *et al*., 2001; Gopalswamy *et al*., 2005; Vršnak, 2001; Vršnak *et al*., 2002; Vršnak *et al*., 2004; Vršnak *et al*., 2007 and others like Dal Lago *et al*., 2004; Howard *et al*., 2007; Lindsay *et al*.,1999; Schwenn *et al*., 2005; Webb *et al*., 2000; Webb *et al*., 2000a). In order to show the comparison between our results and these models, we have plotted in Fig. 8 the travel time versus the ICMEs velocities, considering different cases for the drag force. The thick dark green line is the solution for the laminar regime, with η_1, the thick light green line represents the same regime but with η_2. The turbulent regime travel times are plotted with dot lines, light blue for C_{d1} and violet for C_{d2}. In the case of coupled (laminar plus turbulent) regime, the pink dash line corresponds to coefficients η_1 and C_{d1}. The red dash line corresponds to the same regime but with coefficients η_2 and C_{d2}.

When using the low values of the coefficients (η_1 and C_{d1}) the travel times are similar. On the other hand, the travel time profiles change significantly when using the high value coefficients (η_2 and C_{d2}). In order to compare our results with some empirical models, we have plotted the (Gopalswamy *et al*., 2000) model (thick black continuous line) and the (Gopalswamy *et al*., 2001) modified model (thin black continuous line). We can see that the empirical model (Gopalswamy *et al*., 2001) is in good agreement with our result for the laminar regime at the higher limit (using a viscous coefficient of 0.02 *kg/ms*).

Independently of the values of the coefficients (drag or viscous), it is easy to see that in all cases, the ICME has a damp (more accentuated when the coefficients have higher values) this fact supports the idea of a kind of viscous interaction between the ICME and the interplanetary solar wind. This interaction produces the deceleration of the structure to an asymptotic value of 400 *km/s*, which corresponds to the ambient solar wind velocity.

Fig. 8 shows that our simple and systematic analytical approach may represent the ICME dynamics as well as

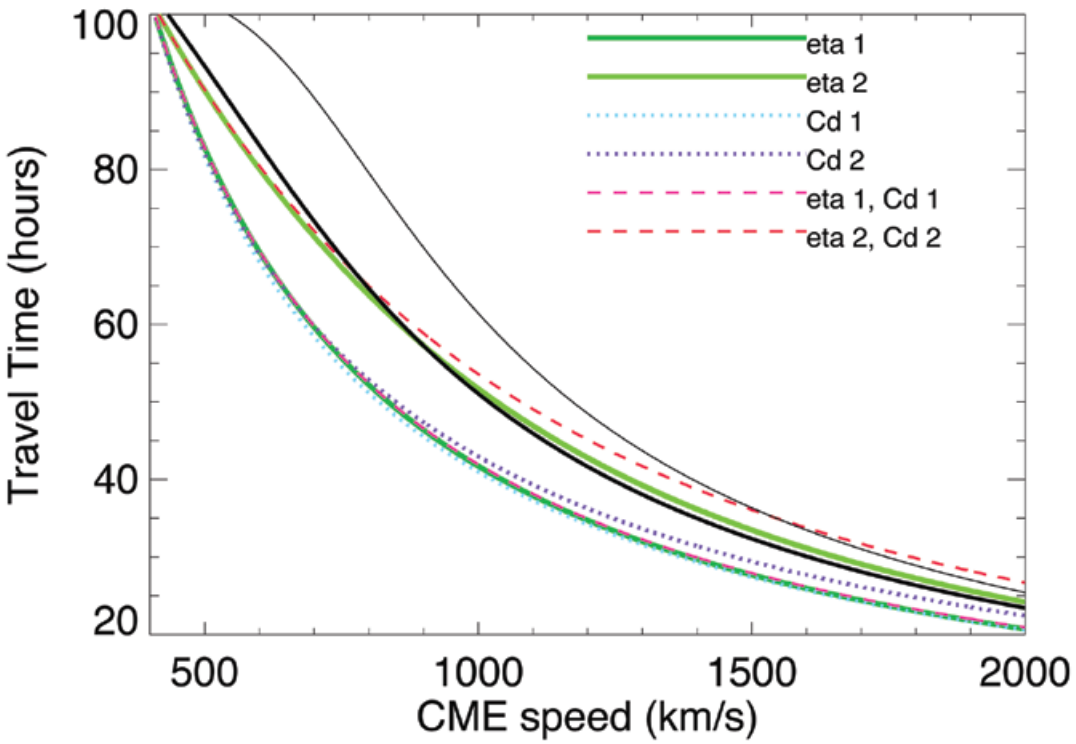

Fig.8. This figure shows the time-travel covered by the ICME as a function of its velocity comparing our results for different and values with respect to empirical models (Gopalswamy *et al*., 2000; Gopalswamy *et al*., 2001).

the empirical models. We are reproducing, in a quite good shape, through a theoretical model, the results claimed by Gopalswamy *et al*. (2000) and Gopalswamy *et al*. (2001). Nevertheless, it is necessary more observational data, along the whole ICME path between the Sun and Earth to validate our model.

Conclusion

In this work we present preliminary results of the study of the momentum exchange between ICMEs and solar wind from the point of view of the fluid dynamics considering the ICME and the solar wind as two interacting fluids with viscous interaction. We have tested the ICME dynamics using a lineal, quadratic and polynomial (order 2) drag forces. We have found values for both the viscosity and drag coefficient to be of the order of $0.002\ kg/ms \leq \eta \leq 0.02\ kg/ms$ and $200 \leq C_d \leq 2000$.

Our model can reproduce the observed difference between the CME velocity observed near the Sun and the ICME velocities observed near 1 AU. Also, this model is able to reproduce in a qualitatively good shape an empirical model for the ICME travel time. Even thought we did not take into account the magnetic field, this hydrodynamic approximation could be used as a first approximation to the understanding of the ICME dynamics.

Acknowledgments

A. Lara thanks UNAM-PAPIT grant IN118906 and CONACyT grant 49395 for partial support.

A. Borgazzi thanks CAPES for financial support.

Bibliography

Batchelor, G. K., 2000. An Introduction to fluid dynamics. Cambridge University Press.

Canto, J., R. F. Gonzalez, A. C. Raga, E. M. de Gouveia Dal Pino, A. Lara, A. and A. Gonzalez-Esparza, 2005. The dynamics of velocity fluctuations in the solar wind I. Coronal mass ejections. Mon. Not R. *Astrom. Soc., 357*, 572-578.

Cargill, P. J. and J. Chen, 1996. Magnetohydrodynamics simulation of the motion of a magnetic flux tubes through a magnetized plasma. *J. Geophys. Res., 101,* A3, 4855-4870.

Cargill, P. J., 2004. On the aerodynamic drag force acting on interplanetary coronal mass ejections. *Sol. Phys., 221*, 135-149.

Dal Lago, A., E. A. Vieira, E. Echer, W. D. Gonzalez, A. L. Clúa de Gonzalez, F. L. Guarnieri, N. J. Schuch and R. Schwenn, 2004. Comparison between halo CME expansion speeds observed on the Sun, the related shock transit speeds to Earth and the corresponding ejecta speeds at 1 AU. *Sol. Phys., 222*, 323-328.

Gonzalez-Esparza, A., A. Lara, E. Perez-Tijerina, A. Santillan, N. Gopalswamy, 2003. A numerical study on the acceleration and transit time of coronal mass ejections in the interplanetary medium. *J. Geophys. Res., 108*, A1.

Gonzalez, W. D., B. Tsurutani and A. L. Clúa de Gonzalez, 1999. Interplanetary origin of geomagnetics storms. *Space Sci. Rev., 88*, 529-562.

Gopalswamy, N., A. Lara, S. Yashiro, M. L. Kaiser and H. Russell, 2001. Predicting the 1-AU times of coronal mass ejections. *J. Geophys. Res., 18*, 29.207-29.217.

Gopalswamy, N., A. Lara, R. P. Lepping, M. L. Kaiser, D. Berdichevsky and O. C. St. Cyr, 2000. Interplanetary acceleration of coronal mass ejections. *Geophys. Res. Lett., 27*, 145-148.

Gopalswamy, N., A. Lara, P. Manoharan and R. Howard, 2005. An empirical model to predict the 1-AU arrival of interplanetary shocks. *Adv. Space Res., 36*, 2289-2294.

Gosling, J. T., D. J. McComas, J. L. Phillips, S. J. Bame, 1999. Geomagnetic Activity Associated with Earth passage of interplanetary Shock disturbance and Coronal Mass Ejections. *J. Geophys. Res., 96*, *A5*,7831-7839.

Gosling, J. T., 1993. Coronal mass ejections:The link between solar and geomagnetic activity. *Phys. Fluids B, 5, issue 7*, 2638-2645.

Howard, T. A., C. D. Fry, J. C. Johnston and D. F. Webb, 2007. On the evolution of coronal mass ejections in the interplanetary medium. *Astrophys. J., 667,* 620-625.

Lindsay, G. M., J. G. Luhmann, C. T. Russell, J. T. Gosling, 1999. Relationships between coronal mass ejection speeds from coronagraph images and interplanetary characteristics of associated interplanetary coronal mass ejections. *J. Geophys. Res., 104,* A6, 12515-12523.

Odstrič̆l, D. and V. J. Pizzo, 1999. Distortion of the interplanetary magnetic field by three-dimensional propagation of coronal mass ejection in a structured solar wind. *J. Geophys. Res., 104,* A12, 28225-28239.

Odstrič̆l, D. and V. J. Pizzo, 1999. Three-dimensional propagation of coronal mass ejections (CMEs) in a structured solar wind flow I. CME launched within the streamer belt. *J. Geophys. Res., 104,* A1, 483-492.

Odstrič̆l, D. and V. J. Pizzo, 1999. Three-dimensional propagation of coronal mass ejections (CMEs) in a structured solar wind flow II. CME launched adjacent to the streamer belt. *J. Geophys. Res., 104,* A1, 493-503.

Schwenn, R., A. Dal Lago and W. D. Gonzalez, 2005. The association of coronal mass ejections with their effects near the Earth. *Ann. Geophys., 23*, 1033-1059.

St. Cyr, O. C., J. T. Burkepile, A. J. Hundhausen and A. R. Lecinski, 1999. A comparison of ground-based and spacecraft observations of coronal mass ejections from 1980-1989. *J. Geophys. Res., 104,* A6, 12493-12506.

Vandas, M., S. Fisher, M. Dryer, M. Smith and T. Detman, 1995. Simulation of magnetic cloud propagation in the inner heliosphere in two-dimensions I. A loop perpendicular to the ecliptic plane. *J. Geophys. Res., 100,* A7, 12258-12292.

Vršnak, B., 2001. Dynamics of solar coronal eruptions. *J. Geophys. Res., 106,* A11, 25249-25259.

Vršnak, B. and N. Gopalswamy, 2002. Influence of the aerodynamic drag on the motion of interplanetary ejecta. *J. Geophys. Res., 107*, A2.

Vršnak, B., D. Ruždjak, D. Sudar, N. Gopalswamy, 2004. Kinematics of coronal mass ejections between 2 and 30 solar radii. *A&A, 423*, 717-728.

Vrnšak, B. and T. Žic, 2007. Transit times of interplanetary coronal mass ejections and the solar wind speed. *A&A, 472*, 937-943.

Webb, D. F., R. P. Lepping, L. F. Burlaga, C. E. DeForest, D. E. Larson, S. F. Martin, S. P. Plunkett, D. M. Rust, 2000. The origim and development od the May 1997 magnetic cloud. *J. Geophys. Res., 105*, A12, 27251-27259.

Webb, D. F., E. W. Cliver, N. U. Crooker, O. C. St. Cyr, and B. J. Thompson, 2000. Relationship of halo coronal mass ejections, magnetic clouds, and magnetic storms. *J. Geophys. Res., 105*, A4, 7491-7508.

A. Borgazzi[1*], A. Lara[2], L. Romero-Salazar[3] and A. Ventura[2,3]

[1]Divisão de Geofísica Espacial, Instituto Nacional de Pesquisas Espaciais, São Jose dos Campos, São Paulo, Brazil, National Institute for Space Research Geophysics Space Division, Av. Dos Astronautas 1758 - Jd. da Granja, São Paulo, Brazil

[2]Instituto de Geofísica, Universidad Nacional Autónoma de México, Del. Coyoacán, 04510 Mexico City, Mexico

[3]Facultad de Ciencias, Universidad Autónoma del Estado de México, Mexico City, Mexico.

E-mail: alara@geofisica.unam.mx

**Corresponding author: andrea@dge.inpe.br*